Supporting Information

Boosting Oxygen Migration via Plasmons of Au Nanoparticles in the Solar-driven Solid Oxide Photoelectrolysis Cells

Jinhao Mei[1], Guangyu Deng[1], Chenge Chen[1], Shiyao Wu[1], Yanwei Zhang[1,], Chenyu Xu[1,**]*

State Key Laboratory of Clean Energy Utilization, Zhejiang University, Hangzhou 310027, China

* Tel.: +86-571-87952040; Fax: +86-571-87951616; E-mail address: zhangyw@zju.edu.cn

** Tel.: +86-571-87952401; E-mail address: mrxcy@zju.edu.cn

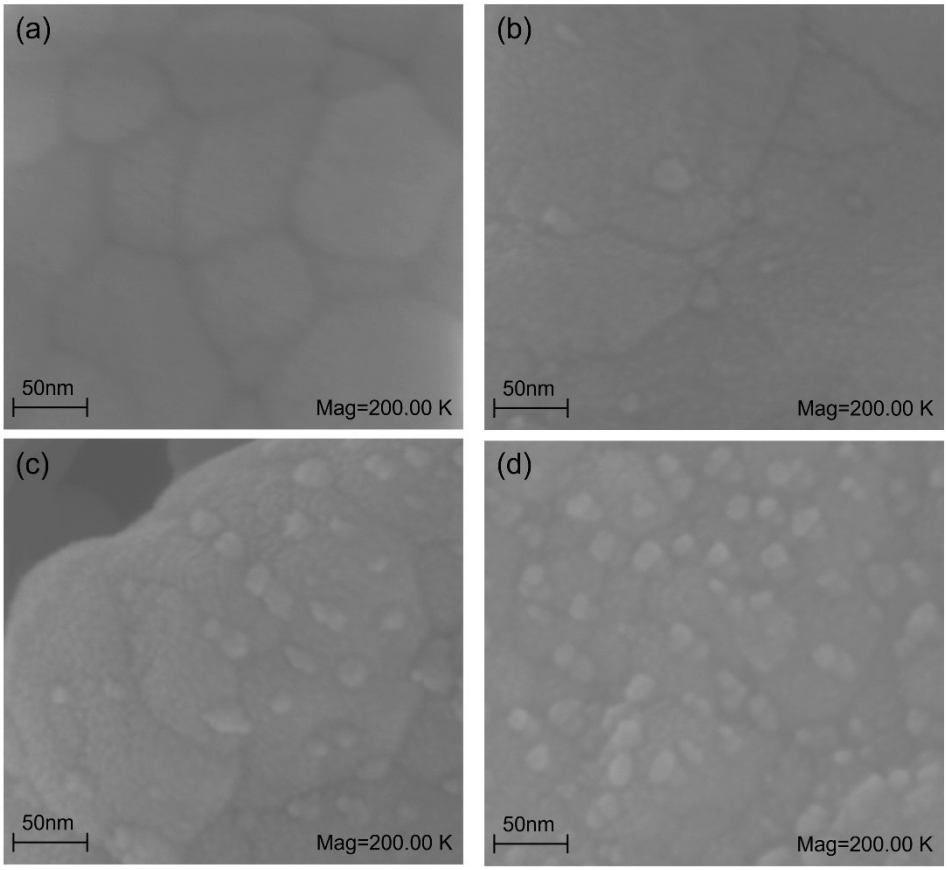

Fig. S1. The high-magnification SEM images of (a) LST, (b) Au40-LST, (c) Au80-LST and (d) Au120-LST.

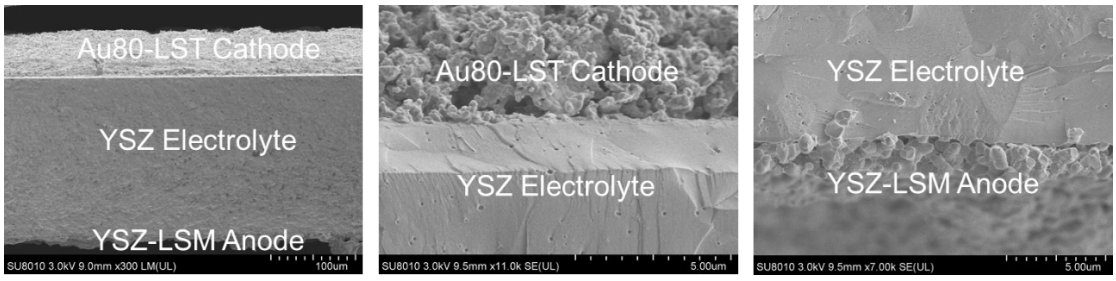

Fig. S2. SEM images of cell cross-section view.

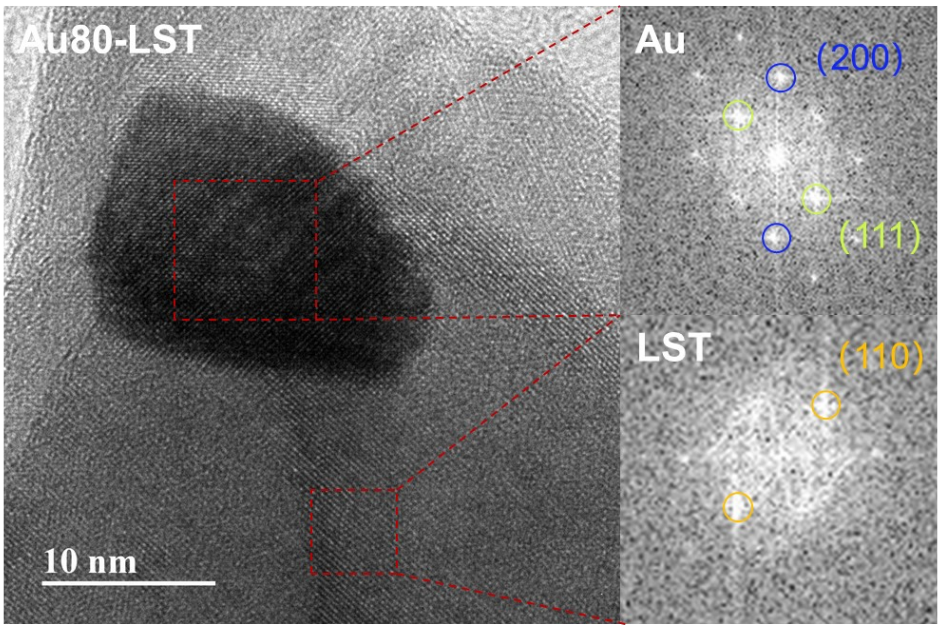

Fig. S3. HRTEM images of Au80-LST.

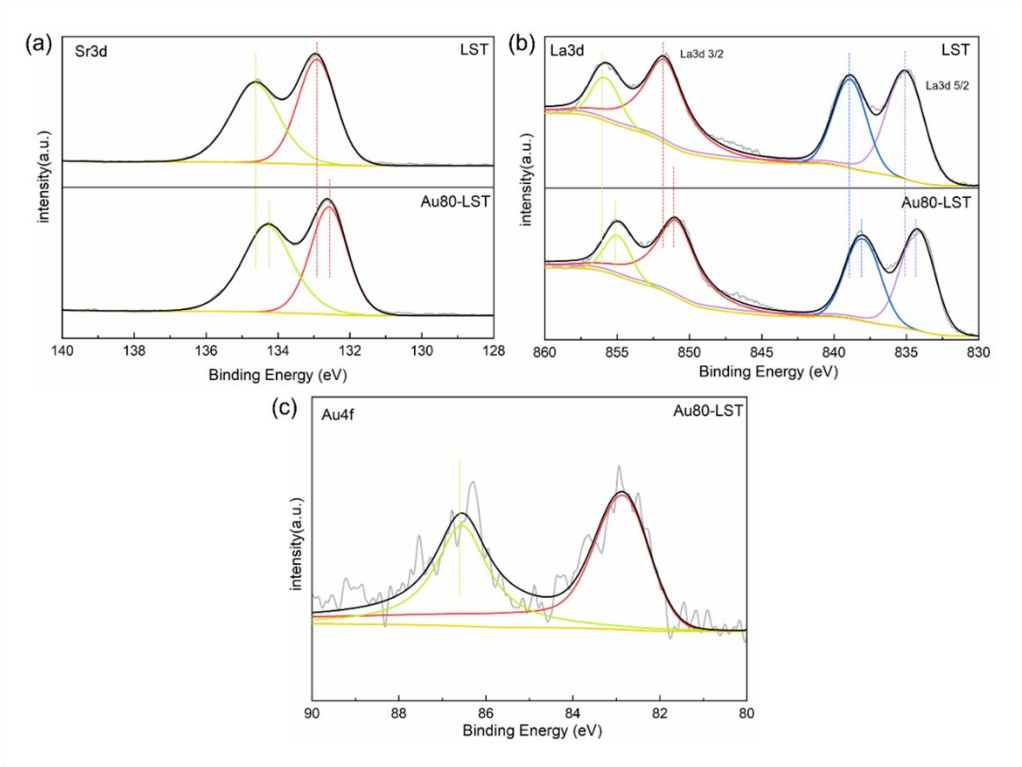

Fig. S4. XPS spectra of (a) Sr3d orbital; (b) La3d orbital for LST and Au80-LST; (c) Au4f orbital for Au80-LST.

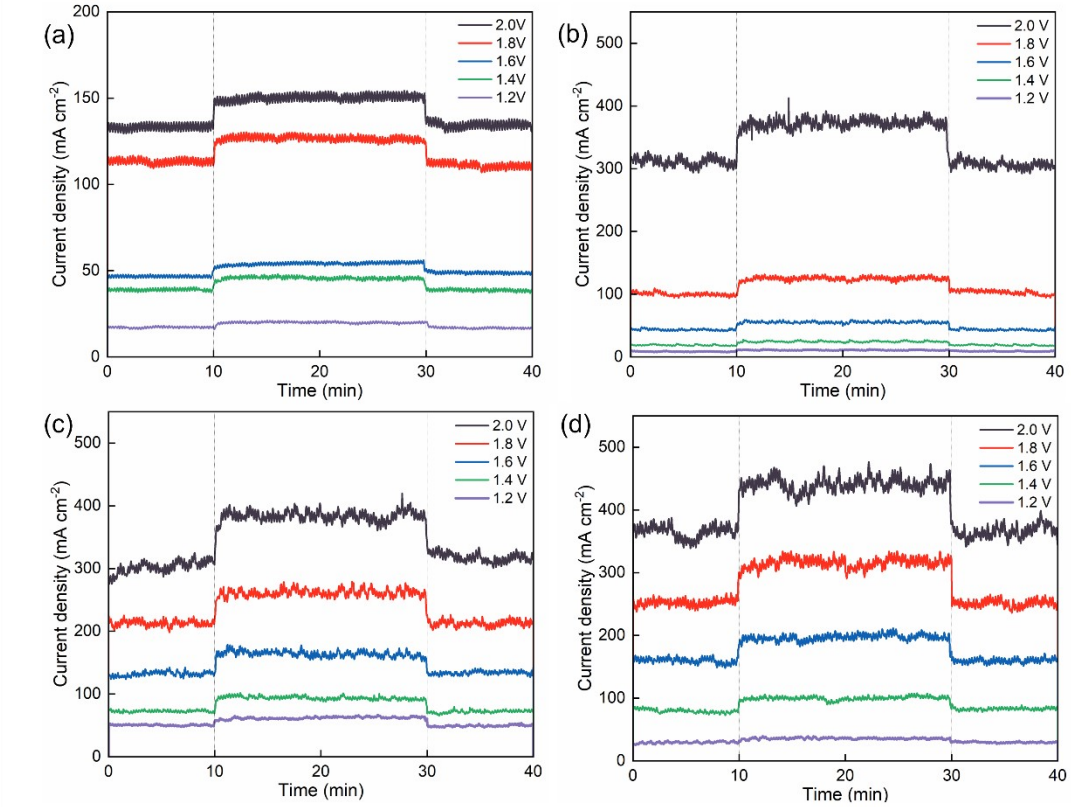

Fig. S5. In alternating light-dark experiments conducted at different constant voltages, the current values of cathodes with different Au contents under the same light source. (a) LST (b) Au40-LST (c) Au80-LST (d) Au120-LST.

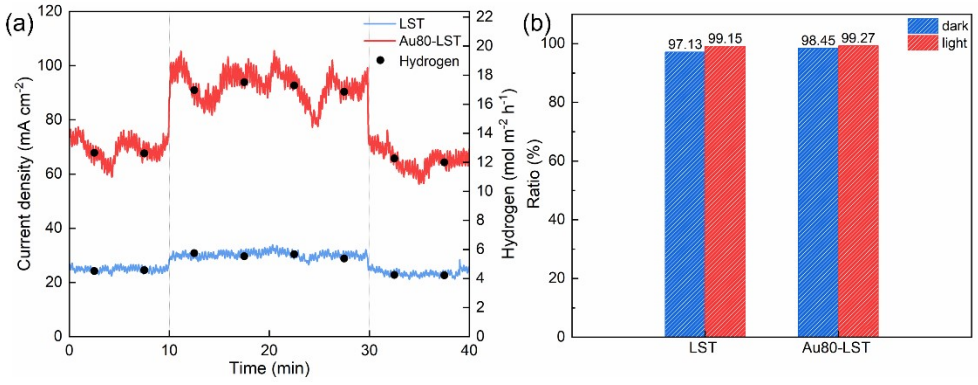

Fig. S6. (a) Gas tests of LST and Au80-LST in alternating light-dark experiments; (b) Faradaic efficiencies of LST and Au80-LST under light and dark conditions.

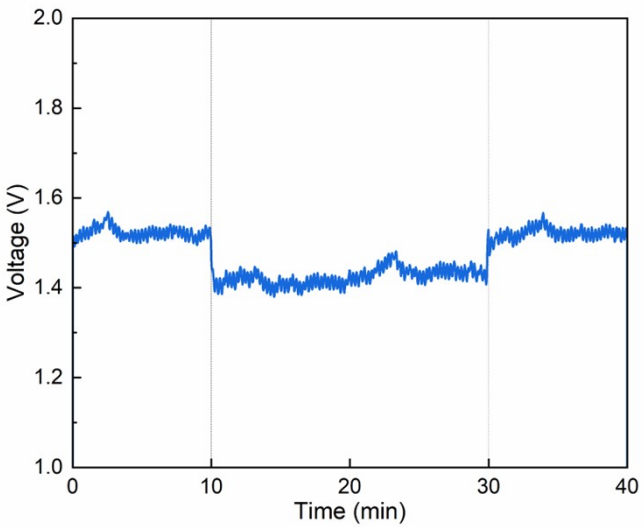

Fig.S7. Constant current test of Au80-LST at 100 mA/cm^2 under alternating light and dark conditions.

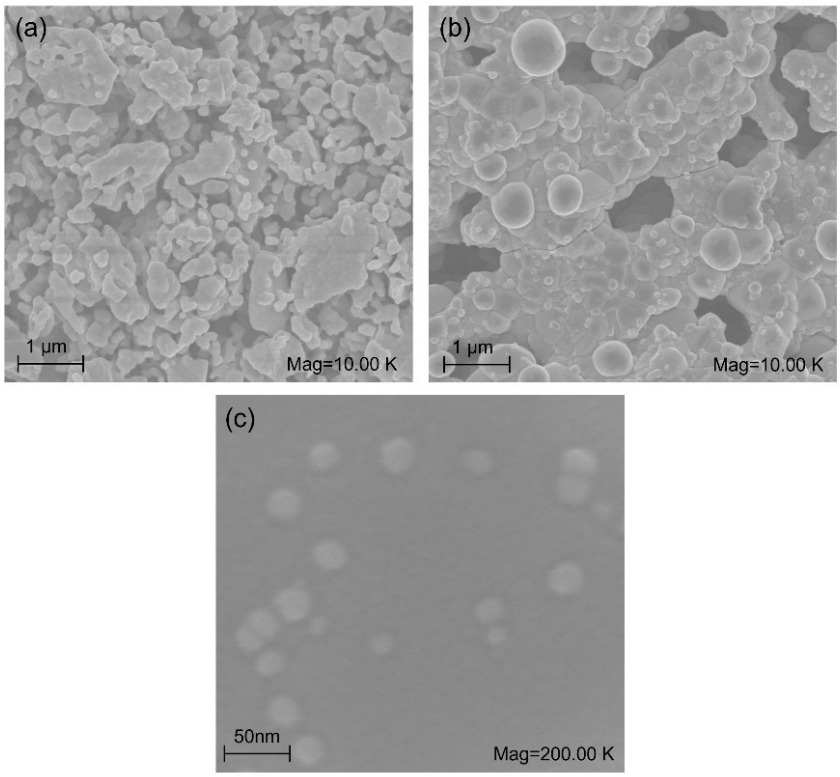

Fig.S8. Low magnification SEM images of Au80-LST before and after long-term SOPC testing: (a) before the experiment; (b) after the experiment; (c) High magnification SEM images of Au80-LST after long-term SOPC testing.

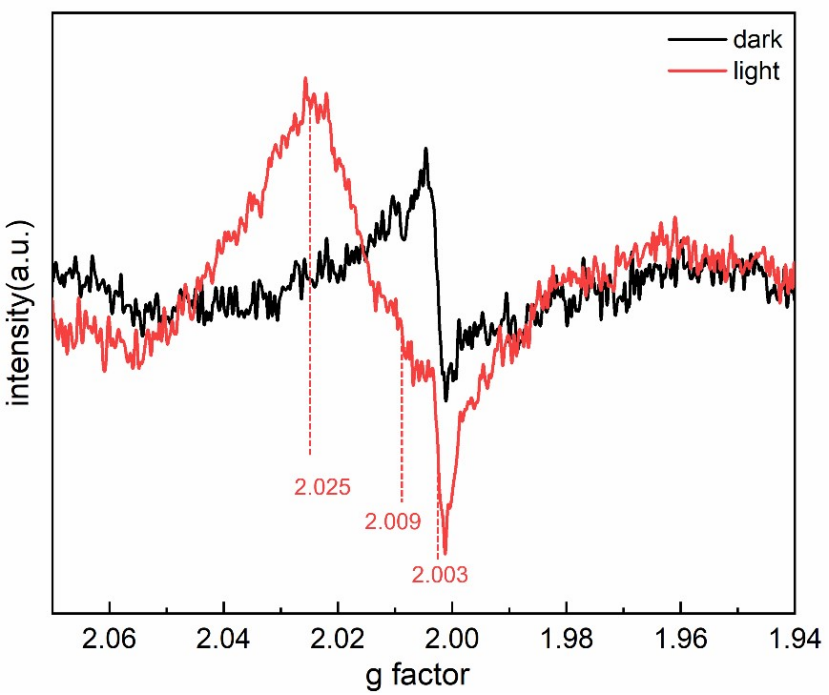

Fig.S9. EPR spectra of Au80-LST in dark and light condition.

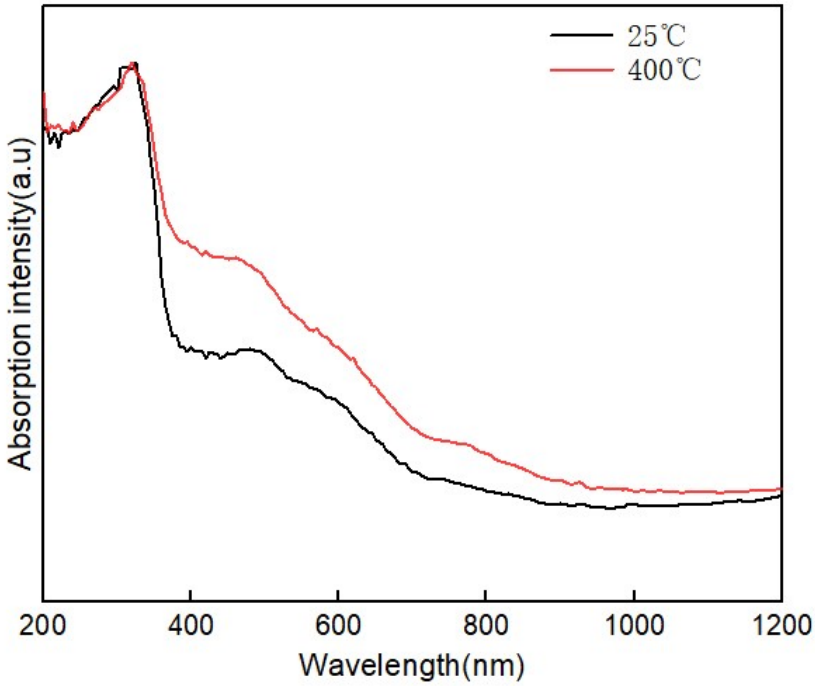

Fig. S10. Variable temperature UV-Vis spectra of Au80-LST.

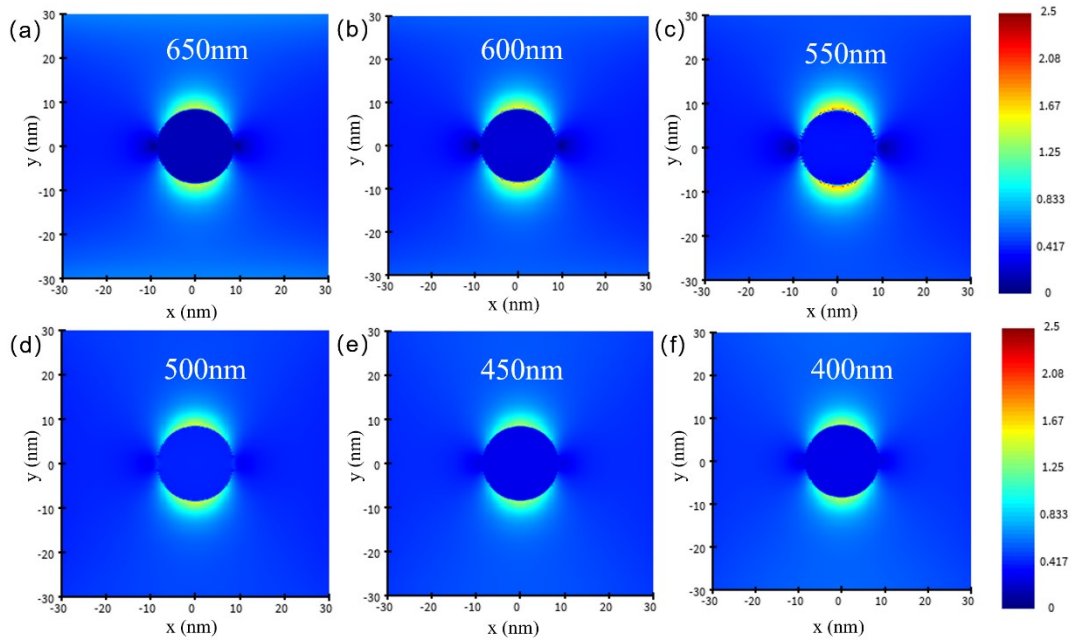

Fig. S11. Top view of the wavelength-dependent FDTD simulation on the Au(17nm)-LST.

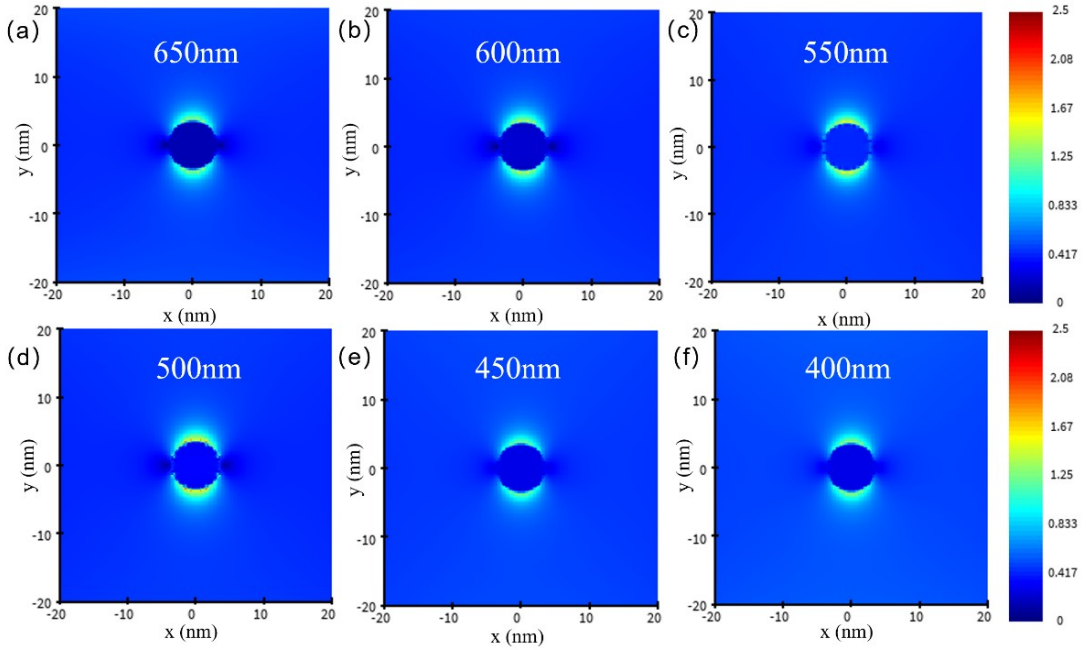

Fig. S12. Top view of the wavelength-dependent FDTD simulation on the Au(7nm)-LST.

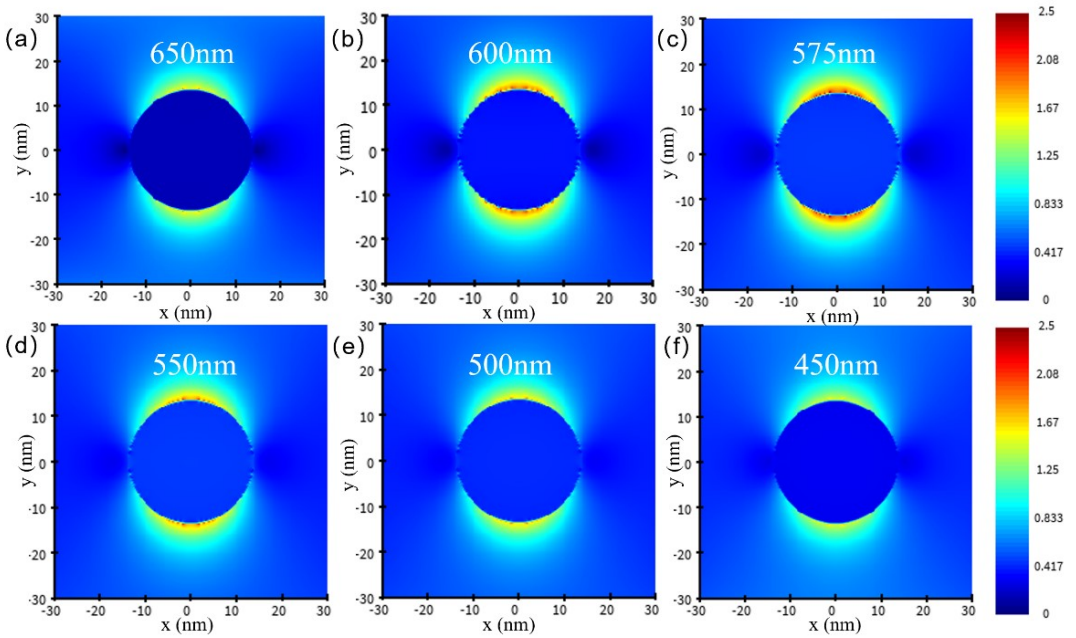

Fig. S13. Top view of the wavelength-dependent FDTD simulation on the Au(27nm)-LST.

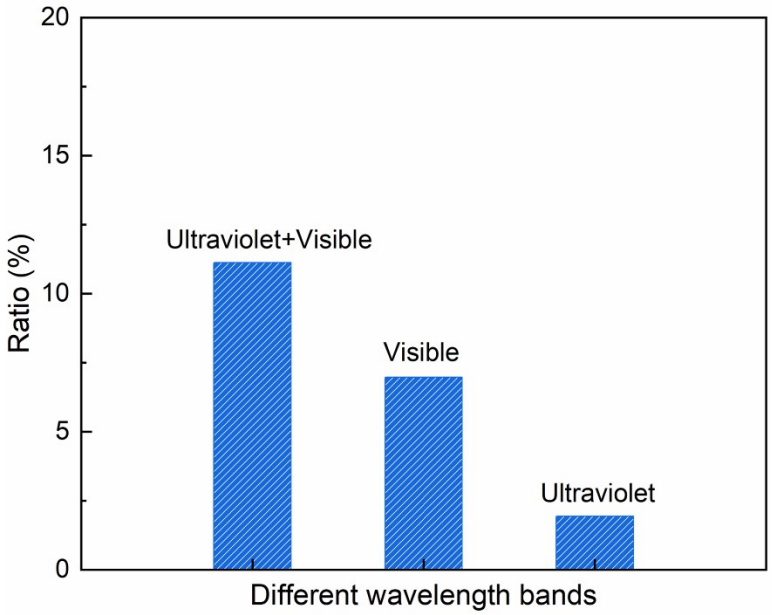

Fig. S14. Variable wavelength experiments for the infrared-depleted (<700 nm), visible, and ultraviolet (<400 nm) light regions at 1.4V.

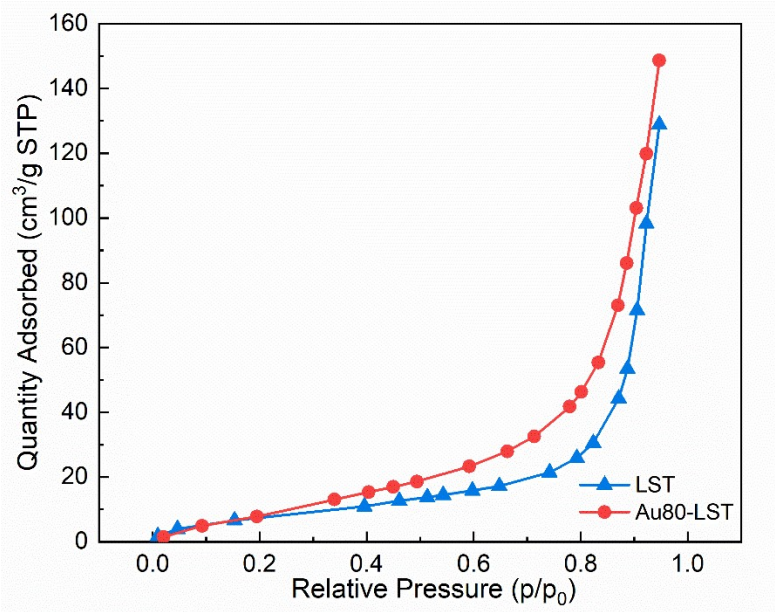

Fig. S15. BET analysis of LST and Au80-LST.

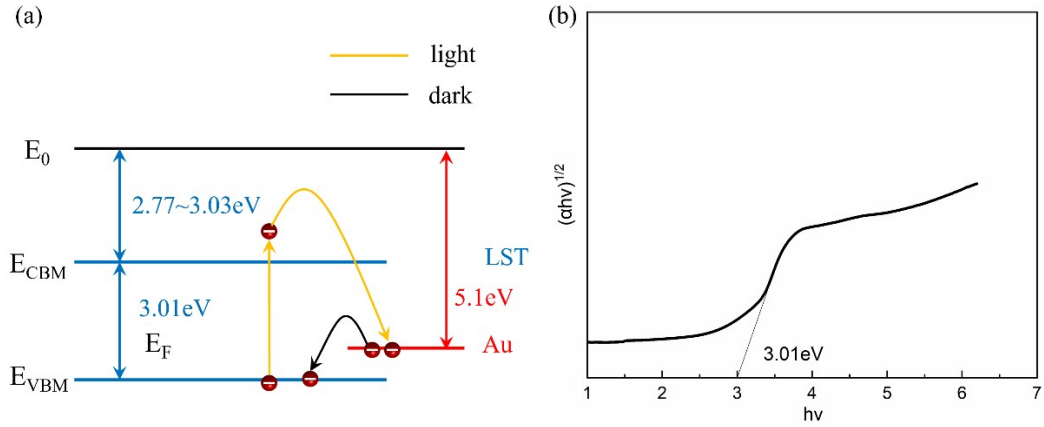

Fig. S16. (a) Energy band positions of LST and Au relative to the vacuum level; (b) Tauc plots of LST.

Table S1. Comparison of works on similar photocatalytic system.

Photocatalysts	Sacrificial Agent	H_2 evolution rate	References
Au-$La_{0.3}Sr_{0.7}TiO_3$	/	14.01 mol/(h*m^2)	This work
Cd@Al_2O_3@ZnO	Sodium sulfide, Sodium sulfide	1.19 mol/(h*m^2)	1
RhCrCo-$SrTiO_3$:Al	/	2.55 mol/(h*m^2)	2
CdS/o-Co_2P	88 vol% lactic acid	184.48 mmol/(h*g)	3
$Ni_{12}P_5CdS$	Na, Na_2SO_3	13.89 mmol/(h*g)	4
Ti_3C_2MXene/ TiO_2/$CuInS_2$	Methanol	356.27 μmol/(h*g)	5
Ni@NiS_X-CdS	Na_2S and Na_2SO_3 aqueous solution	78.7 mmol/(h*g)	6
UiO-66/WP	TEOA, EY	384 mmol (5h)	7
$Zn_{0.5}Cd_{0.5}S$/Ni_2P	Na_2S and Na_2SO_3 aqueous solution	21.19 mmol/(h*g)	8

References

1 D. Ma, Z. Wang, J.-W. Shi, Y. Zou, Y. Lv, X. Ji, Z. Li, Y. Cheng and L. Wang, *J. Mater. Chem. A*, 2020, **8**, 11031–11042.

2 Y. Xie, C. Xu, Y. Liu, E. Zhang, Z. Chen, X. Zhan, G. Deng, Y. Gao and Y. Zhang, *Adv. Sci.*, 2025, **12**, 2410201.

3 Y. Chao, J. Zheng, H. Zhang, F. Li, F. Yan, Y. Tan and Z. Zhu, *Chem. Eng. J.*, 2018, **346**, 281–288.

4 X. Guo, J. Cao, M. Guo, H. Lin, Y. Chen and S. Chen, *Catal. Commun.*, 2019, **119**, 176–179.

5 W. Yang, G. Ma, Y. Fu, K. Peng, H. Yang, X. Zhan, W. Yang, L. Wang and H. Hou, *Chem. Eng. J.*, 2022, **429**, 132381.

6 X. Zhang, F. Wu, G. Li, L. Wang, J. Huang, A. Meng and Z. Li, *Appl. Catal. B: Environ.*, 2024, **342**, 123398.

7 Z. Jin, Y. Zhang and Q. Ma, *J. Colloid Interface Sci.*, 2019, **556**, 689–703.

8 S. Dhingra and C. M. Nagaraja, *Int. J. Hydrog. Energy*, 2018, **43**, 22917–22928.